Conference on

Machine Processing of

Remotely Sensed Data

October 16 - 18, 1973

The Laboratory for Applications of
Remote Sensing

Purdue University
West Lafayette
Indiana

CLASSIFICATION OF TURBIDITY LEVELS IN THE TEXAS MARINE COASTAL ZONE

E. A. Weisblatt, J. B. Zaitzeff and
C. A. Reeves

Lockheed Electronics Company, Inc., Houston, Texas;
National Oceanic and Atmospheric Administration,
Rockville, Maryland; and
Lockheed Electronics Company, Inc., Houston, Texas

I. ABSTRACT

The unsupervised Iterative Self-Organizing Clustering System (ISOCLS) and the supervised Earth Resources Interactive Processing System (ERIPS) were used to detect, delineate and classify near-surface turbidity patterns in the Galveston and Trinity Bays, Texas and adjacent coastal waters. Data used in the analysis was ERTS-1 Multispectral Scanner (MSS) digital data in the visible spectral bands from 0.5 to 1.1 micrometers, and related in situ water measurements.

Theoretical considerations suggest that because solar radiation attenuates with water depth and water constituents as a function of wavelength, classification of turbidity levels based on spectral characteristics is a classification based on spectral signatures from varying water depths; that is, a classification of spatially different points. In classification of turbidity therefore, combinations of spectral radiance in several visible and near infrared bands should yield varying geographic patterns.

An experiment was designed to 1) study turbidity classification utilizing ERTS-1 multispectral scanner data, and 2) to calibrate spectral reflectance with turbidity levels. Preliminary results indicate theoretical and empirical compatibility in classification using a single channel of information and the potential for ground calibration of the ERTS-1 multispectral scanner data measurement of turbidity. Additionally it was found that turbidity induces linearity in 2 channels for the distribution of water as a class and that the unsupervised ISOCLS classification procedure handled the non Gaussian distribution better than the ERIPS supervised technique of classification.

II. INTRODUCTION

Practically all coasts of the world possess examples of rapidly filling estuaries. When the oceans reached their present level, about 3000 years ago, estuarine sedimentation began its most recent geomorphic episode. Common to most estuaries today are prograding deltaic systems at river mouths; growing marshes, tidal flats and beaches; dynamic bottom topographies; and highly turbid waters, all of which are products of the sedimentation process.

In response to current trends in the use of estuaries for navigation of commercial vessels, fishing, breeding grounds, sewage disposal, port development, and recreation, considerable effort in marine sicence and coastal engineering has been expended on the development of physical models to predict sedimentation and circulation patterns. Few models consider remotely sensed data as significant inputs. It is evident to these authors that the remotely sensed, and automatically processed data generated by the Earth Resources Technology Satellite-1 (ERTS-1), and the NASA Data Analysis Stations (DAS) can contribute significantly to the measurement of near surface turbidities in highly turbid estuaries. It is not difficult to envision the eventual integration of such data into more complex three dimensional physical models of water turbidity. Accurate classification of near surface turbidity levels and circulation patterns, therefore, represents only a primary step in predictive model development.

This paper illustrates several examples of both supervised and unsupervised classifications of waters in Galveston Bay, Texas, which are characterized by turbidities ranging between 20 and 120 parts per million (ppm) and also evaluates the use of the ERTS-1 multispectral scanner data in turbidity predictions. In addition, 4 channel EXOTECH radiometric data collected and correlated empirically with water turbidities in four surveys of Galveston Bay are analyzed. The results of the water survey analysis strongly influence the method of classification and are consistent with radiative transfer laws.

III. ERTS-1 DATA ANALYSIS

In the analysis procedure bulk ERTS-1 multispectral data taken from several passes over Galveston Bay, Texas area were received from the Goddard Space Flight Center and converted through a sequence of format changes to 7 track LARSYS II computer compatible tapes. During the preprocessing procedure several areas of Galveston Bay were selected, screened and edited for cluster analysis and maximum likelihood classification. Computer printout, cathode ray tube (CRT), and film positive options were available for display of the clustering and classification results. The digital data processing flow is diagrammed in Figure 1.

III. UNSUPERVISED CLASSIFICATION

The unsupervised Iterative Self-Organizing Cluster Analysis System (ISOCLS) is designed to define the means or centers of spectral clusters in "n" dimensional spectral space of registered data sets. A cluster is the multichannel space that is usually associated with spectrally homogeneous features in the data.

Inputs to the ISOCLS algorithm consist of the data to be clustered, the maximum number of clusters to be defined (MAXCLS), the maximum allowable standard deviation (STDMAX) for nominal cluster splitting, a threshold value for combining or chaining clusters (DLMIN), and the maximum number of allowable iterations (ISTOP). Other inputs are feasible and will be described in greater detail in another paper in this conference (Kan, E.P.F., et al, 1973).

During the initial iteration of the program all data points fall into a single cluster, or into some predefined set of clusters according to a distance measure, D_1. The distance measure is computed as the sum of the absolute differences between the given point coordinates and the given cluster center coordinates taken each channel separately, i.e., the distance D_1 is defined as $\sum_{i=1}^{m} \bar{x}_i - x_i$ where $\bar{x}_i$ is the cluster mean of the ith channel and x_i is the point position in the ith channel. After the points are assigned to the various cluster means, the mean and standard deviation in each channel is recomputed for each set

of cluster data. If any one or more of the standard deviations for all channels of data exceeds the STDMAX, that is exceeds the nominal cluster size, for more than 20 percent of the clusters, then the subject clusters are split in the band that exhibit the largest standard deviation.

After splitting, two new means are defined as $\bar{x} + \sigma_i$ and $\bar{x}_i - \sigma_i$ where σ_i is the old standard deviation in the ith channel. If and when the splitting criteria is satisfied by more than 80 percent of the clusters, the cluster separations are checked to determine if two or more clusters should be combined according to the input value of DLMIN. If the number of members of a cluster is less than 30, then the bluster is eliminated. The iterative process ends when either the number of iterations reaches or exceeds ISTOP, or the number of clusters reaches or exceeds MAXCLS.

Beginning with some specified iteration, a cluster symbol map is printed out for each subsequent iteration. If desired, the ISOCLS clustering program also places the final cluster symbol map data on a computer compatible tape that is formatted in a manner compatible with the CRT display programs of the data analysis station.

III.2 SUPERVISED CLASSIFICATION

The second pattern recognition system used in this study is the Earth Resources Interactive Processing System (ERIPS) which is a maximum likelihood classification capability. In this technique, the analyst spatially defines training areas in an image with the assumption that the training areas define a known class or feature. For each training field, he assigns a field name, a class name, and a class symbol. More than one training field may be defined for one class. In addition the analyst defines test fields and one or more large areas to be classified. The NASA Johnson Space Center uses the LARSYS algorithm as a maximum likelihood classifier.

In the LARSYS algorithm, the means and covariances for each channel among classes and channels are calculated from the digital data defined within the training fields. Then, assuming a normal distribution of points about the mean, the algorithm calculates the normalized probability density function. A threshold value is selected which represents the percentage of points that are to remain unclassified due to their distance in spectral space from the class means. The threshold percentage represents different distances in each channel and each class. A point is assigned to a particular class on the basis of the highest probability of association. The closer the point falls to a mean in "n" dimensional spectral space, the higher the probability that point belongs to that class. When the threshold value is exceeded, the point is assigned to the nonclassified group, i.e. the threshold class. In this way each point is classified into one class.

IV. CLASSIFICATION OF WATER TURBIDITY

Both classificatory systems make assumptions which may not necessarily apply directly to automatic pattern recognition of water turbidity. Theoretical considerations suggest that the intensity of solar radiations attenuated with water depth and water constituent as a function of wave length. Classification of turbidity utilizing spectral signatures therefore is based on light reflecting from varying points in space along the z axis of the geographic coordinate system. In essence water transmits shorter wavelength energy with depth in the visible and near infrared portion of the electromagnetic spectrum and tends to rapidly absorb the longer wavelength energy near the surface.

Figure 2 shows single channel image enhancements of Trinity Bay, which is the largest lobe of Galveston Bay. ERTS-1/MSS channel 4 (500- 600nm) on the upper left side, illustrates six separate density slices. From considerable ground work, the authors know that the red color in the upper right hand corner (Lake Anahuac) represents the most turbid water. In descending order of turbidity, yellow, light brown, green, maroon and blue follow sequentially. MSS channel 6 (700-800nm) on the upper right illustrates only four classes of turbidity. At least a part of the difference in the classes in the two images may be related to upwelling light in channel 4 emanating from depths greater those in channel 6. Although spatial patterns resemble each other, close comparison indicates

pronounced variation along the boundaries of each class where rapid changes in light transmissivity occur. As a result, areal estimates of each class would be grossly inaccurate. An unsupervised ADP classification of Trinity Bay based on two channels shown in Figure 3 would not necessarily correspond to average surface turbidities, but would correspond to turbidities of some average water depth from which light is emanating in each of the two channels. Similarly, a 4 channel classification (Figure 4) represents turbidity patterns over some average depth, whatever that may be. In both cases, turbidity estimates may be accurate over those depths however areal estimates of turbidity by class differ.

A second assumption held by both the unsupervised and supervised classification systems is that each class typically displays a normal Gaussian distribution in each of the 4 ERTS channels. In fact, as shall be shown below, water turbidity tends to correlate either linearly on non-linearly with radiance in each ERTS band, depending on wavelenghths. An assumption of normality in the overall density function of the class water in Galveston Bay does not accurately describe the distribution.

In the case of ISOCLS, the unsupervised clustering algorithm, the lack of normality does not have serious ramifications in classification. Inputting the appropriate STDMAX; that is, the appropriate threshold for splitting clusters results in a chain of small clusters which closely approximates the overall distribution of highly turbid bay waters.

In contrast, the authors experienced unusually poor classification in the supervised, ERIPS, pattern recognition procedure. In approximately 50 percent of the training fields selected, correct classification of picture elements was less than 75 percent (Fig. 5). That is, training fields from which statistics were computed were themselves extremely heterogeneous. Both large and small training fields demonstrated this characteristic. Exceptions seemed to occur commonly in waters of the highest and lowest turbidities.

Difficulties in selecting representative training fields along a turbidity gradient again relate to the variations in light transmissity of the water medium. In a typical analysis, training fields selections occur in a single band displayed on a CRT. This selection corresponds to a particular column of surface water, however 4 channel classifications consider several masses of water. Supervised 4 channel classification therefore is characterized by a twofold problem. In the first case questions arise as to what water mass which is being classified, and second training statistics represent a heterogeneous mixture of turbid water in most cases.

As a result of the questions raised during the preliminary classification attempts, a ground truth program was implemented utilizing the EXOTECH, 4 band, ERTS radiometer. (Fig. 6).

IV.1 GROUND SURVEYS

In our observations of Galveston Bay waters an attempt was made to measure the depths from which light was upwelling in each ERTS channel.

An EXOTECH, ERTS Ground Truth Radiometer, Model 100 was used to measure reflected radiation/over a highly reflecting 3' by 4' white target as it was lowered into water at different locations of varying turbidities. The radiometer is designed to closely replicate the spectral characteristics of the ERTS-1 MSS by providing four separate channels of data for analysis. Each bandpass function is shown in Figure 7 and subsequent figures show the relative relationships of the instrument response. Several inferences may be made about Galveston Bay waters from this experiment.

Figure 8 shows the relative attenuation of target reflectance in the 600-700nm band as a function of water depth in waters of differing turbidities and sun angles. The curves typify the nature of light in turbid water and agree conceptually with the work of earlier investigators.

Light attenuation is greatest near the surface/for all turbidities and reflected energy wavelengths. Between 60 and 70 percent of the subaerial target reflectance in Galveston Bay attenuates in that band within 1.0 foot of the

surface. By approximately 2.0 feet or less, depending on sun angle, the curves become asymptotic. The asymptote represents the depth at which the target no longer induces a response on the instrument; that is, it represents the depth at which all solar radiation incident on the target is either absorbed, scattered, or reflected in the water medium. Similar response curves occur for other turbidities and instrument bandpasses, although rates of light upwelling decay were rapid in long wavelength bands as theory and empirical measures show. The target, for example, induced a small response in the 700-800 nm and 800-1100 nm (EXOTECH) bands at depths exceeding one foot (Figure 9) which is apparently contrary to reports that all light at near infrared wavelengths of the ERTS radiometer is absorbed in the first few centimeters. In both channels however, one foot of water had diminished, probably by absorption, between 85 to 95 percent of the target's reflected energy. In comparing the long and short wavelength response, the reader should recall that the bandpass in the 800-1100 nm band is approximately twice that of the other bands. Had the data been normalized to a common bandpass width, the relative relationship would force the response to be about 1/2 the value shown.

According to Fresnel's equation, as zenith angles increase, reflectance from a smooth surface increases, first slowly, then beyond 35°, rapidly. This increase in reflectance would not only lower the total incident solar radiation entering the water, but would also alter the asymptoteof the attenuation curves to a lower value. This assumption was tested in the early morning sun in a small, protected harbor of Galveston Bay. Sun zenith angle equalled 60°. Turbidity values of 24 ppm at the test station were among the lowest encountered in the estuary. Although the 24 ppm curve in Figure 8 takes the characteristic form, incident energy was about 40 percent less that the other curves and the asymptote was reached at about the 1.75 foot water depth. In contrast, the other curves measured on the same day at zenith angles less than 30° and in water of higher turbidities show that the asymptote shifted to about 2.0 feet as indicated above.

Several investigators considering distilled water or sea water of low turbidity have determined empirically, the physical characteristics of light in a water medium. Clark and James (1969), measuring the transmittance properties of distilled water, show that peak transmittance of light in water occurs in a band between 440 and 560 nanometers. This band corresponds closely to measurements of transmittance of open sea water and clear fresh water made earlier by Hulbert (1945) and more recently by Ross (1969), Tyler and Smith (1970), Duntley (1963), Jerlov (1968), and Williams (1970).

In all water of low turbidity, total downwelling irradiance tends to drop sharply with increasing water depth, the peak transmittance band narrows, and the attenuation of light is greatest in the red and infrared portion of the reflecting spectrum. As turbidity of water reaches high levels, similar trends in transmittance occur, however, two prominent deviations become apparent. Attenuation of downwelling irradiance is greatly increased in some proportion with turbidity density and particle size, and peak transmittance shifts toward longer wavelengths. Hulbert (1945) for example, shows the relationship in undefined bay water and notes that peak transmittance occurs at about 550 nm. Few other measurements of light transmittance in highly turbid water have been observed by these authors in the literature, and the relationships are apparently not well defined across the visible and infrared spectrum.

Based on our observations of radiance as the target was lowered in Galveston Bay and the work of earlier investigations, we concluded that for the range of turbidities considered, the radiometric response is some integrated function of light scattering upward from depths not exceeding 2.0 feet in EXOTECH channel 2, and 1.25 feet in channels 1 and 3, and .75 feet in channel 4.

IV.2 REFLECTION AS A FUNCTION OF TURBIDITY

Typically, as turbidity increases, the intensity of upwelling light increases. The measured relationship between instrument response and turbidity for Trinty Bay on three different days is shown in Figure 10. A HACH turbidometer was used to measure water turbidity at 103 stations throughout the bay during three surveys. Most readings of turbidity and water reflectance were made in the time period between 10:00 AM and 3:00 PM, corresponding roughly to sun angles varing within 35° of zenith. Clear to slightly hazy atmospheric conditions occurred on the third survey day. The data clearly displayed greater variance in instrument

response on the cloudy day and average radiance measurements were higher than clear days. A slight cloud-day effect was felt in all channels in the correlation analysis between turbidity and radiance.

Several characteristics of the four scattergrams in Figure 10 deserve note. EXOTECH instrument readings in channels 1 (500-600 nm) and 2 (600-700nm) suggest a strong linear response to water turbidity. Correlation coefficients for each channel equalled .88 and .92 respectively and both showed highly significant F ratios at the .05 level of significance. In contrast channel 3 (700-800mn) yields a curvilinear response which is more pronounced in channel 4 (800-1100mn). Measured turbidity values in the range between 20 and 70 ppm in channel 4 (i.e. values left of the dashed line) induced no change in radiance. One implication of this response is simply that in the lower turbidity range, infrared energy is quickly absorbed in the surface layers, but as turbidity levels approach certain thresholds, upwelling infrared radiance from suspended particulates exceeds the energy absorbed by the surface water. In the range between 70 and 120 ppm instrument response becomes increasingly linear.

Although EXOTECH channel 3 responds to turbidity in a manner similar to channel 4, its threshold occurs at approximately 55 ppm. Additionally the lower range of turbidities displays a very low, rather than flat, slope. The surveyed data suggest that the low slope may be related to the cloudy-day measurements although this point was not fully explored by the authors.

To determine which combination of channels would best predict water turbidity, a stepwise, multiple linear regression was performed on the EXOTECH data. The regression program is designed to select initially, the variable with the highest partial linear correlation with the dependent variable and then all in a stepwise manner, the independent variables which induce the greatest reduction in the error sums of squares. This process is equivalent to explaining the variance found in the distribution of turbidity measurements, by sequentially considering the radiance measured in each of the EXOTECH channels.

Channel 2 (600-700 nm) was the first variable entered and channels 4 (800-1100 nm), 3 (700-800 nm) and 1 (500-600 nm) followed sequentially. Channel 2 explained 83.91 percent of the variation in water turbidity. After adding all four variables, only 84.45 percent of turbidity variance was explained - an increase of less than 1 percent.

The explanation of this result lies, in part, in the high correlations between channels, all of which exceeded .80. Channels 1 and 2 correlated better than all others (.969) however, a students-t test indicated that the partial regression relationships were different at the .01 level of significance. Channel 3 also correlated highly with channel 2, indicating that it also may effectively discriminate turbidity levels over the 20 to 120 ppm range.

As a primary result of the multiple regression analysis, channel 2 (600-700nm) was selected as the best ERTS-1 channel for turbidity prediction, and that the other channels enhance predictions in only a minor way. Furthermore, each of the other channels have standard errors of estimates which exceed that of channel 2.

Assuming that the EXOTECH instrument response closely resembles that of the ERTS-1 MSS radiometers, certain obvious deductions may be made about the enhanced images of Galveston Bay shown in Figure 2. First, turbidity levels exceed approximately 55 ppm in channel 3 and 70 ppm in channel 4. Second, the energy sensed emanated from a maximum of 1.25 feet water depths in channel 3 and a 0.75 feet maximum water depth in channel 4. Similarly energy sensed in channels 1 and 2 correspond to maximums of 1.25 feet and 2.0 feet respectively. Of the four channels, channel 2 best represents the full 20-120 ppm range of turbidity by virtue of the strong linear relationship and highly significant correlation existing in the data.

Finally, note should be made of the distribution of spectral radiance of the class "water". EXOTECH data indicate that none of the ERTS channels display a Gaussian distribution, however, within turbidity levels, normality may occur because of the natural variation in the sediment characteristics. Thus, a pattern recognition technique should consider water turbidity in small modular units corresponding to turbidity levels.

IV.3 TEST SITE RESULTS

During the course of the analysis four sets of data were studied. Figure 2 for example, represents an ERTS-1 data set gathered on January 19, 1973. In that figure, each channel is treated individually. Turbidity in ERTS-1 channel 6 (700-800 nm) does appear only in those areas of highest particulate concentration in the bay and Lake Anuhuac. Similarly, channel 7 (800-1100 nm) shows turbidity differentiation only at the highest points of sediment concentration. Qualitatively, these data support the trends implied by the ground surveyed data. Similar trends were observed in all data sets.

A second data set was tested more rigorously with actual ground measurements on May 8, 1973 (Figure 11). Data collected within two hours of the ERTS-1 overpass were correlated with the ADP image classifications. Both supervised (ERIPS) and unsupervised (ISOCLS) ADP systems were tested. In the former case seven turbidity level training fields were defined in a channel 5 (600-700nm) CRT, black-and-white image. In the 4 channel classification of training fields, four of the seven yielded under 75 percent correct classifications of picture elements within a "single class". A 2 channel classification (500-600 nm and 600-700 nm bands) resulted in only slight improvement of training field classification. Because of the difficulties in selecting training fields along the turbidity gradient, the supervised procedure was no longer considered in our analysis.

A total of seven water turbidity classes were discriminated in the unsupervised (ISOCLS) procedure using a 1.0 STDMAX. The relationship between the midclass value of turbidity and the average ERTS-1 image radiance was computed (Figure 12). Although only six points are available to demonstrate the relationship between turbidity and radiance in each channel, essentially the same trends as those of the ground data occur. Channels 4 (500-600 nm) and 5 (600-700 nm) display a linear relationship and 6 (700-800 nm) and 7 (800-1100 nm) a curvilinear function. Unfortunately, the few points available were insufficient to statistically demonstrate the relationship with high levels of significance.

Four unsupervised classifications of turbidity were attempted on the May 8 data set. Three classifications considered all 2 channel combinations of ERTS-1 MSS (Figure 13) and a 4 channel classification. Classification results indicated that the channel 4/channel 5 classification separated turbidity classes, but failed to discriminate several water classes from several land classes, thus was ineffective as an ADP classifier of a land and water scene. Use of channels 6 and 7 in conjunction with channel 5 separate water classes from land classes however, the channel 5/7 classification did not provide a adequate picture of the turbidity classes. Of each combination, the channel 5 and channel 6 combination best represents turbidity classes.

In evaluating individual ERTS-1 channels of the May 8 data set, (Figure 14) it was found that channels 4 and 5, yield nearly identical results in terms of class discriminations. Whereas channel 6 also discriminated most of the range of turbidity on that day (approximately 55 ppm to 115 ppm), turbidities below about 80 ppm are not well defined and class separation is difficult. Similarly, channel 7 discriminated only the highest turbidity levels, thresholding to a constant graytone at some point below 115 or 120 ppm.

V. CONCLUSIONS

ERTS-1 multispectral scanner data are capable of discriminating water turbidity levels covering the range of 20 to 120 ppm observed in this study. Supervised classification programs utilized were found to be somewhat ineffective in selecting spectrally homogeneous water training fields. The unsupervised classification algorithms were determined to be a more accurate technique for water classification. Of the four ERTS-1 channels available for classification, channel 5 (600-700 nm) and 6 (700-800 nm) yielded the most accurate results when compared with in situ measurements of water turbidities.

The authors wish to acknowledge the suggestions and efforts of the Coastal Analysis Team in general and Dr. Jack Paris in particular. This team was one of six teams assembled by NASA and LEC to evaluate the ERTS-1 remote sensing system.

REFERENCES

Clark, G. L. and James H. R., "Laboratory Analysis of the Selective Absorption of Light by Sea Water", *Journal of the Optical Society of America*, 29:43-53, February 1969.

Duntley, S. Q., "Light in the Sea", *Journal of the Optical Society of America*, 53:214-33 February 1963.

Hulburt, E. O., "Optics of Distilled and Natural Water", *Journal of the Optical Society of America*, 35(11):698-705 November 1945 or 24:35-42 1945.

Jerlov, N. G., *Optical Oceanography*, Elsevier Rub. Co. Amsterdam, 1968.

Kan, E. P., W. A. Holley, and H. D. Parker, "The JSC Clustering Program ISOCLS and Its Applications", Purdue University, 1973.

Ross, D. S. et. al. "Experiments in Oceanographic Aerospace Photography-I, Ben Franklin Spectral Filter Tests", Philco-Ford Corp; U.S. Naval Oceanographic Office, Cont. No. N62306-69-C-0072 August 1969.

Tyler, J. E. and Smith, R. C., *Measurements of Spectral Irradiance Underwater*, Gorden and Breach 1970.

Williams J., "Optical Properties, of the Sea", U.S. Naval Instruction, Annapolis, Maryland 1970.

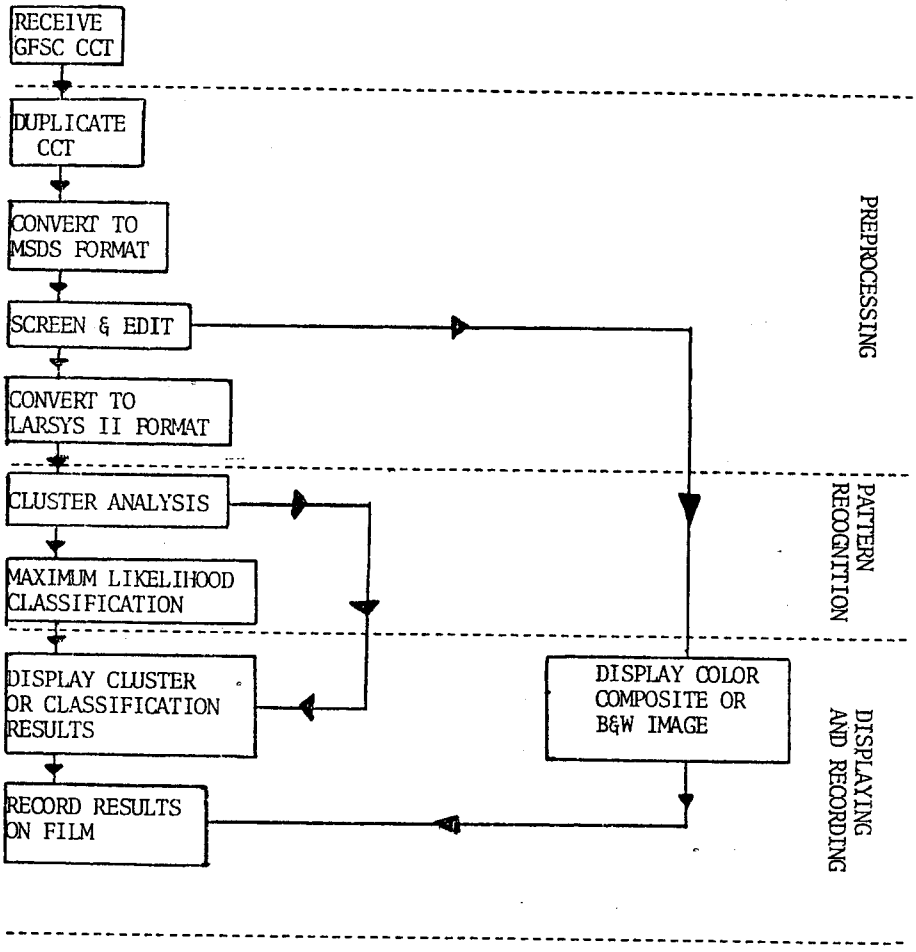

FIGURE 1. DIGITAL DATA FLOW DIAGRAM

500 - 600 nm

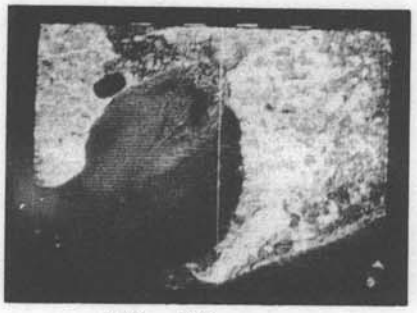

700 - 800 nm

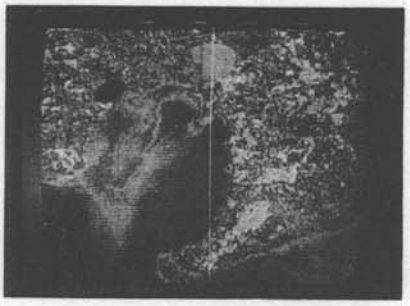

600 - 700 nm

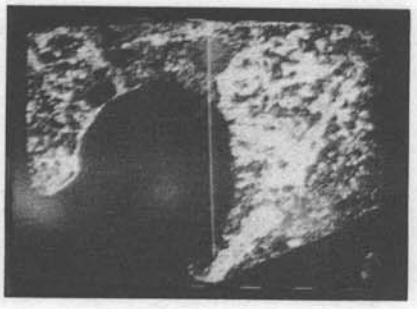

800 - 1100 nm

FIGURE 2. IMAGE ENHANCEMENTS OF ERTS-1 DATA, TRINITY BAY, TEXAS JAN. 19, 1973

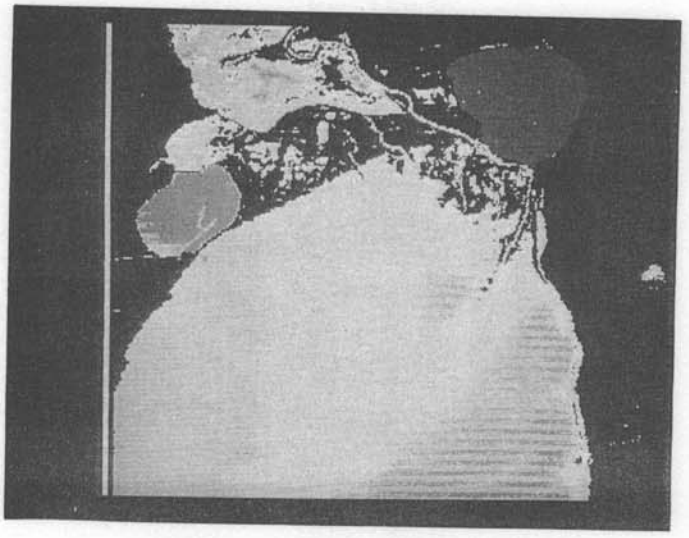

FIGURE 3. TWO CHANNEL CLASSIFICATION
OF WATER TURBIDITY (700-800nm/800-1100nm)

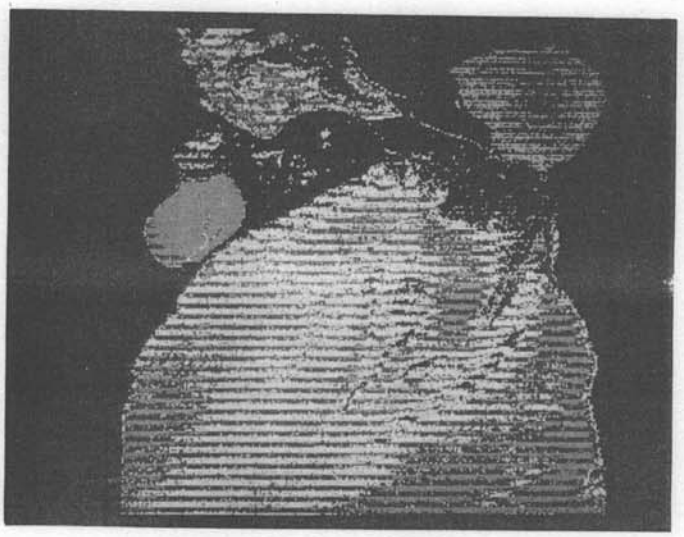

FIGURE 4. FOUR CHANNEL CLASSIFICATION
OF WATER TURBIDITY

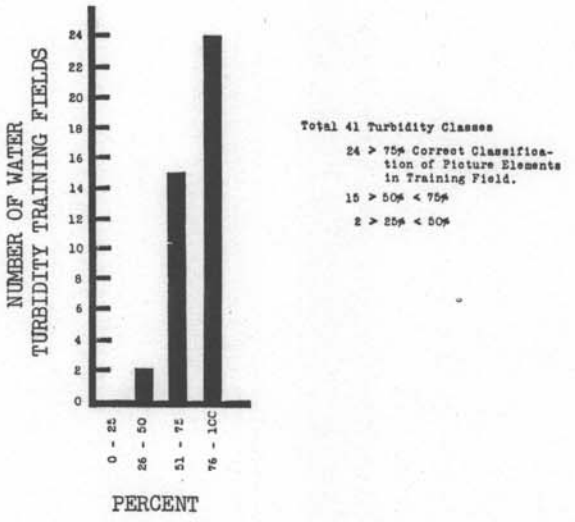

FIGURE 5. PERCENT CORRECT CLASSIFICATION OF PICTURE ELEMENTS CONTAINED IN A SAMPLE OF 41 TURBIDITY TRAINING FIELDS

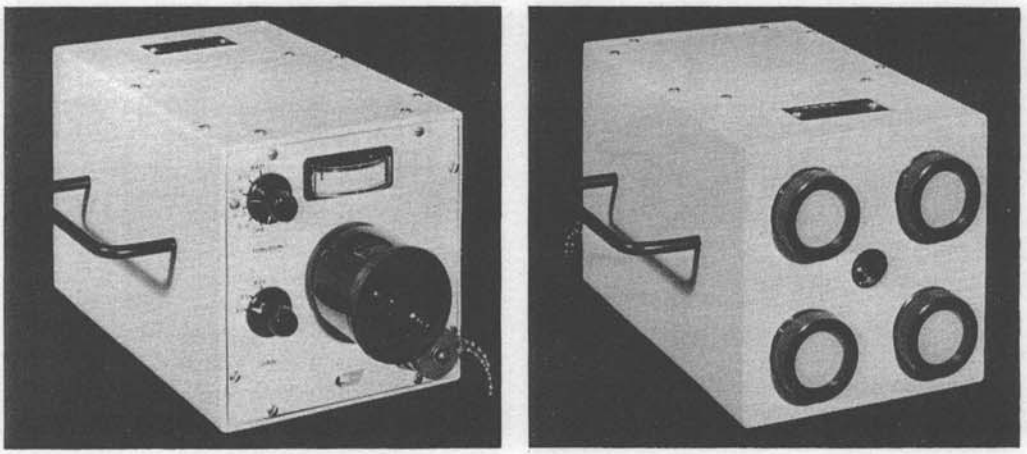

FIGURE 6. EXOTECH RADIOMETER

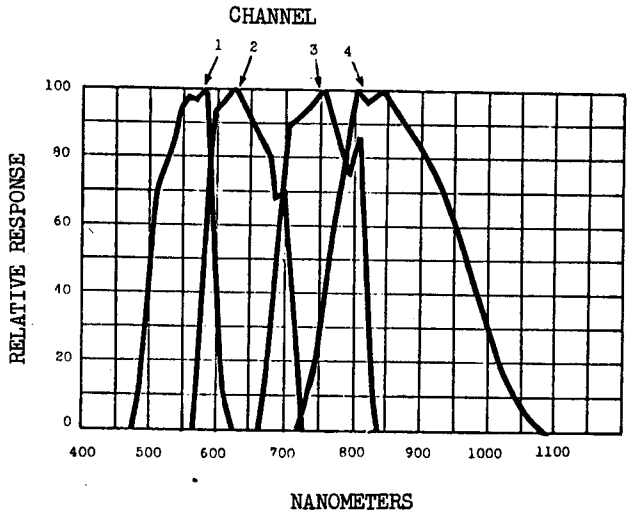

FIGURE 7. EXOTECH BANDPASS FUNCTIONS

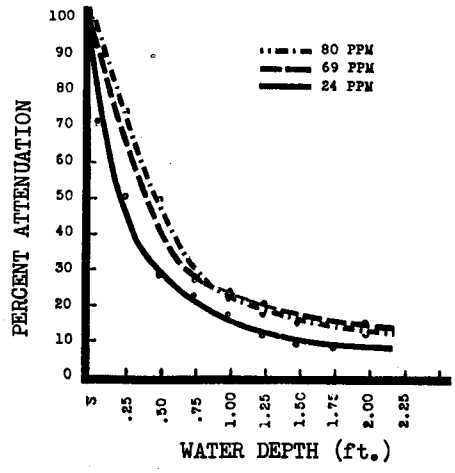

FIGURE 8. PERCENT ATTENUATION OF UPWELLING LIGHT FROM TARGET IN CHANNEL 2

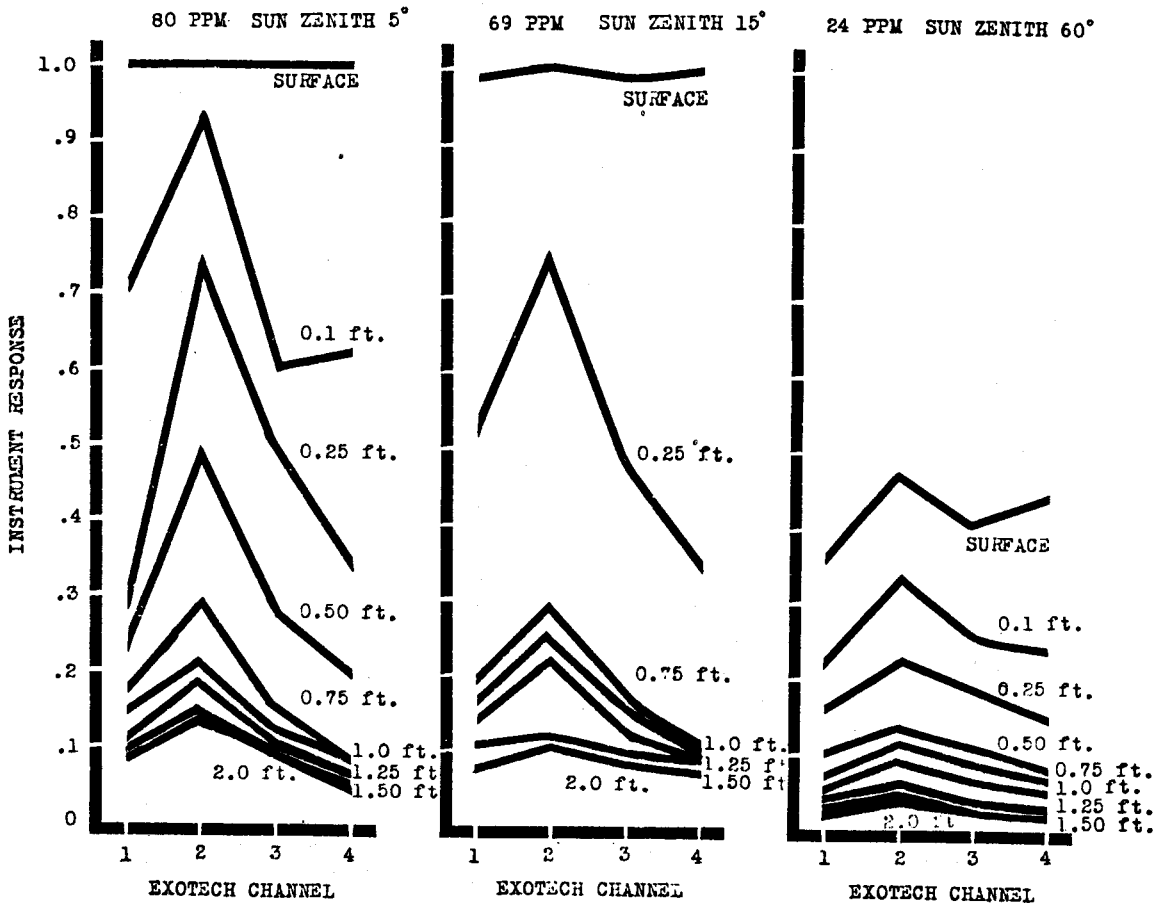

FIGURE 9. INSTRUMENT RESPONSE TO SUBMERGED TARGET

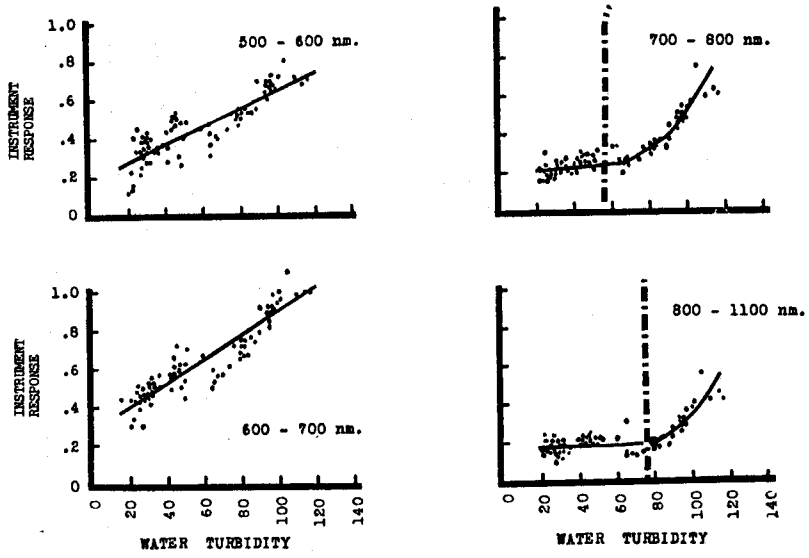

FIGURE 10. INSTRUMENT RESPONSE AS A FUNCTION OF WATER TURBIDITY OF BAY WATERS

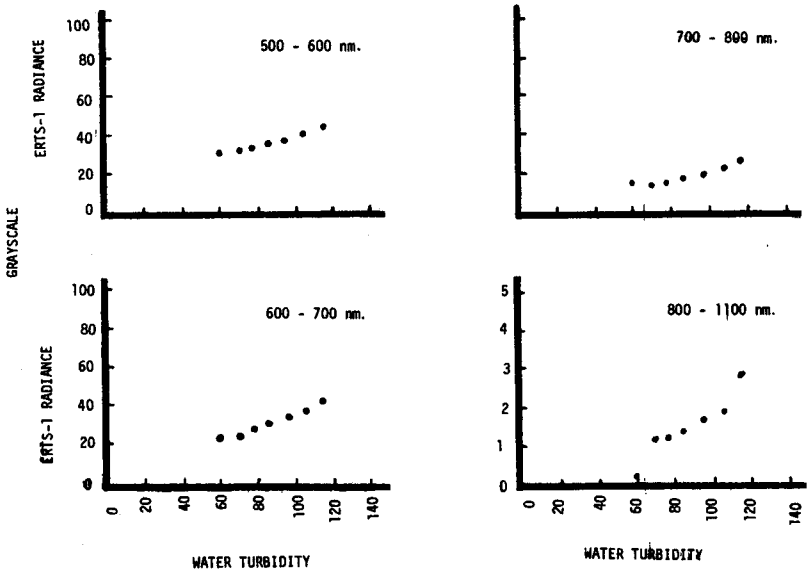

FIGURE 11. ERTS-1 RADIANCE AS A FUNCTION OF WATER TURBIDITY

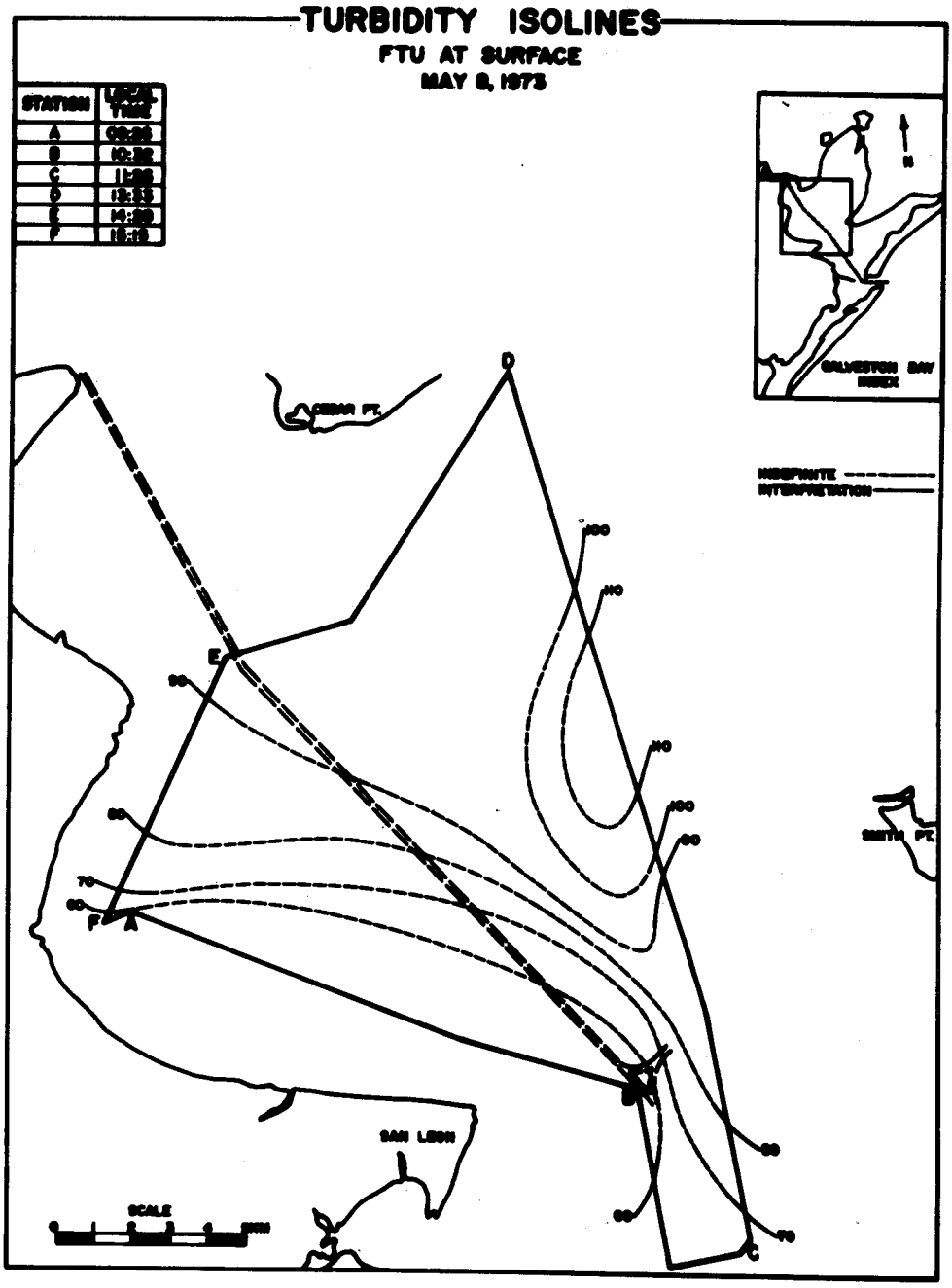

FIGURE 12. TURBIDITY (FTU) TRINITY BAY, MAY, 8, 1973 WATER SURVEY

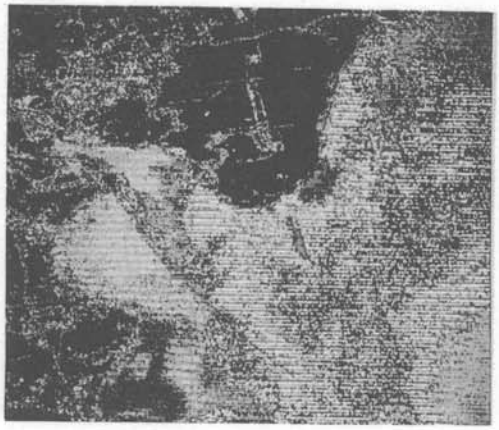

CHANNEL 4/5 CLASSIFICATION

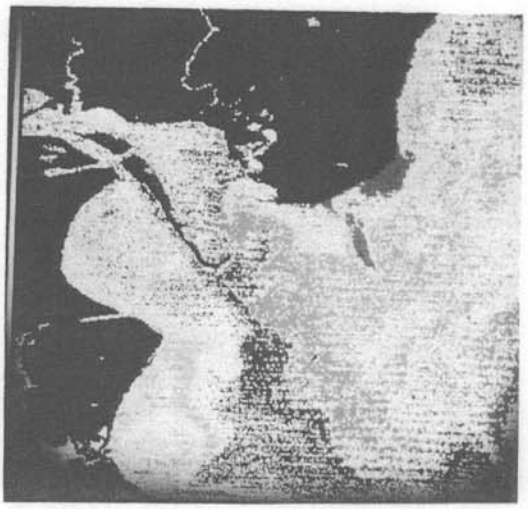

CHANNEL 5/7 CLASSIFICATION

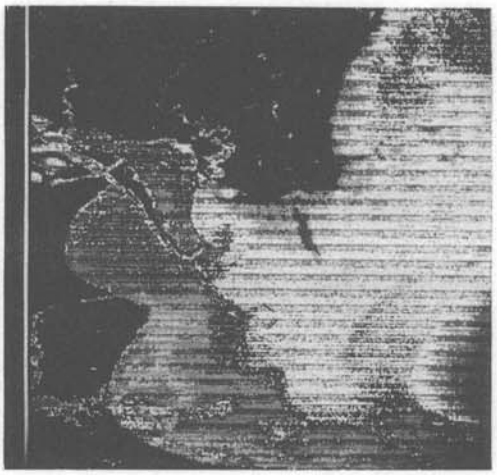

CHANNEL 5/6 CLASSIFICATION

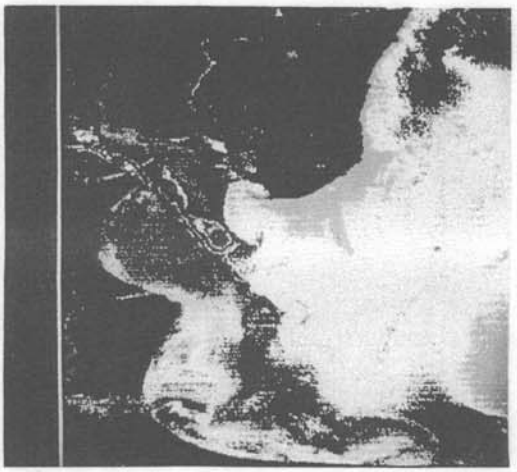

CHANNEL 4/5/6/7 CLASSIFICATION

FIGURE 13. TURBIDITY CLASSIFICATIONS (UNSUPERVISED) OF TRINITY BAY, MAY, 8, 1973

500-600 nm

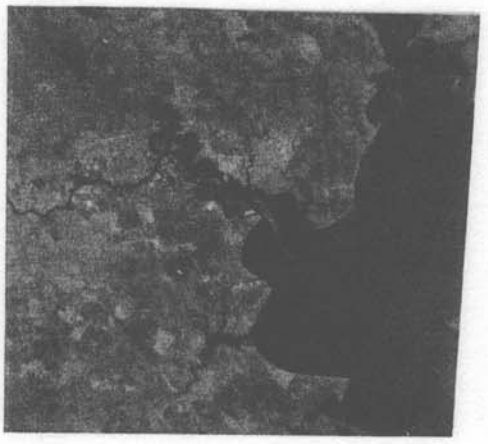

700-800 nm

600-700 nm

800-1100 nm

FIGURE 14. POSITIVE ERTS - 1 IMAGES OF TRINITY BAY, TEXAS, MAY 8, 1973